Chemical Science

ROYAL SOCIETY OF CHEMISTRY

EDGE ARTICLE

View Article Online
View Journal | View Issue

Cite this: *Chem. Sci.*, 2025, **16**, 2898

All publication charges for this article have been paid for by the Royal Society of Chemistry

Rapid (≤25 °C) cycloisomerization of anhydride-tethered triynes to benzynes – origin of a remarkable anhydride linker-induced rate enhancement†

Dorian S. Sneddon, Paul V. Kevorkian and Thomas R. Hoye *

Received 24th October 2024
Accepted 2nd January 2025

DOI: 10.1039/d4sc07232d

rsc.li/chemical-science

The hexadehydro-Diels–Alder (HDDA) reaction is a cycloisomerization between a conjugated diyne and a tethered diynophile that generates *ortho*-benzyne derivatives. Considerable fundamental understanding of aryne reactivity has resulted from this body of research. The multi-yne cycloisomerization substrate is typically pre-formed and the (rate-limiting) closure of this diyne/diynophile pair to produce the isomeric benzyne generally requires thermal input, often requiring reaction temperatures of >100 °C and times of 16–48 h to achieve near-full conversion. We report here that diynoic acids can be dimerized and that the resulting substrate, having a 3-atom anhydride linker (*i.e.*, O═COC═O), then undergoes HDDA cyclization within minutes at or below room temperature. This allows for the novel *in situ* assembly and cyclization of HDDA benzyne precursors in an operationally simple protocol. Experimental kinetic data along with DFT computations are used to identify the source of this surprisingly huge rate acceleration afforded by the anhydride linker: >10^7 faster than the analogous multi-yne having, instead, a CH_2OCH_2 ether linker.

Introduction

The Diels–Alder [4 + 2] cycloaddition is one of the most, arguably the most, venerated reaction in the field of organic chemistry. Its ability to merge two reactive substrates, a diene and a dienophile, to simultaneously introduce up to four contiguous stereocenters affords it considerable utility and versatility. In light of more recent understanding in the realm of cycloaddition chemistry, we can classify other processes as dehydro variants of the classical Diels–Alder reaction, wherein the alkenes that comprise either the diene or the dienophile are instead alkynes.[1] By this definition, the first disclosure of any Diels–Alder-like process is the 1895 report by Michael and Bucher of the condensation and subsequent tetradehydro-Diels–Alder (TDDA) reaction of two equivalents of phenylpropiolic acid (**1**) in refluxing acetic anhydride to efficiently produce the naphthalene–anhydride derivative **4** (Fig. 1a).[2,3] In 1899, Lanser reported a similar transformation using phosphoryl chloride as the dehydrating agent.[4] Baddar and coworkers later carried out a series of experiments in which they established the intermediacy of phenylpropiolic acid anhydride (**2**) in this transformation.[5] It is now recognized that TDDA

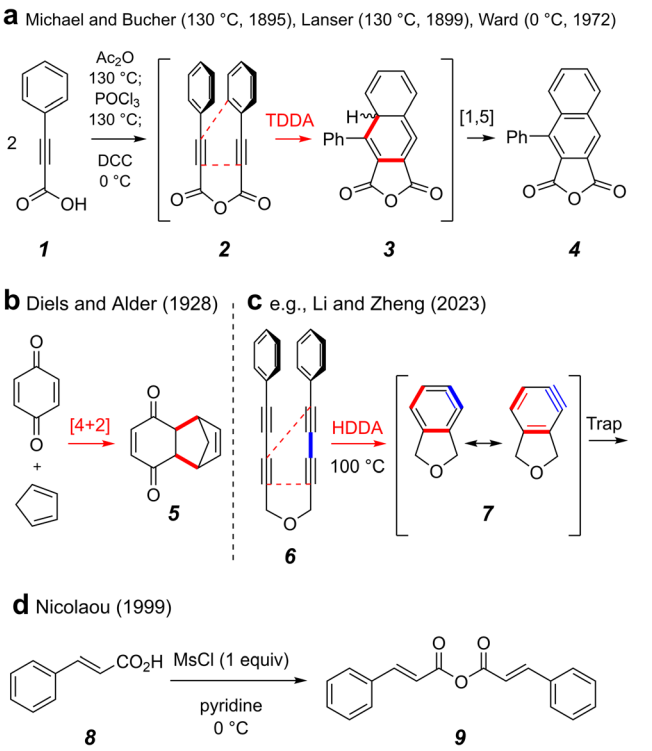

Fig. 1 (a) Reports of the tetradehydro-Diels–Alder (TDDA) reaction of phenylpropiolic acid. (b) A classical Diels–Alder reaction (c). A hexadehydro-Diels–Alder (HDDA) reaction to form an *ortho*-benzyne (and its subsequent trapping). (d) Facile formation of a carboxylic acid anhydride mediated by methanesulfonyl chloride.

Department of Chemistry, University of Minnesota, 207 Pleasant St. SE, Minneapolis, MN 55455, USA. E-mail: hoye@umn.edu

† Electronic supplementary information (ESI) available. CCDC 2353613. For ESI and crystallographic data in CIF or other electronic format see DOI: https://doi.org/10.1039/d4sc07232d

reactions of substrates containing tethered conjugated enyne to alkyne subunits like that present in **2** proceed *via* 1,2,4-cyclohexatrienes **3**,[6] which then undergo net 1,5 H-atom migration to afford **4**.

It was nearly 30 years later that Diels and Alder published their seminal work producing adducts such as **5**, in what we regard today as the classical Diels–Alder reaction (Fig. 1b).[7] A more recent variant of a net cycloaddition reaction to produce six-membered carbocycles is the hexadehydro-Diels–Alder (HDDA) reaction (Fig. 1c).[8] For example, a poly-yne substrate joined by a three-atom tether such as the ether linker in **6** undergoes net intramolecular [4 + 2] cycloaddition to form highly reactive, yet selective, *ortho*-benzyne derivatives such as **7** under purely thermal conditions.[9] Subsequent experiments done by the Ward group[10] in which phenylpropiolic acid (**1**) was converted to the anhydride **2** using DCC were shown to produce the known TDDA adduct **4** even at 0 °C.[11] Considering that most TDDA and HDDA cyclizations proceed by stepwise mechanisms,[12] we reasoned that an anhydride linked multi-yne substrate could potentially produce an HDDA benzyne also at ambient temperature. To date, there are few examples of HDDA substrates that cyclize at or below room temperature.[8,13] One final reaction that influenced our thinking and design of the project we describe here is shown in Fig. 1d. Nicolaou and coworkers described the formation of symmetrical anhydrides under very mild conditions *via* transient, mixed carboxylic–sulfonic anhydrides.[14]

Results and discussion

Two aspects of any HDDA reaction are (i) that it requires the creation of a substrate containing a linked diyne/diynophile pair and (ii) that the rate of generation of the benzyne is fast relative to that of competing side reactions of the substrate and (trapped) benzyne-derived products. In light of the mild reaction conditions sufficient to induce the cyclization of the anhydride **2**, we wondered what temperature would be required to induce HDDA cyclization of an anhydride such as that derived from dehydrative coupling of the conjugated diynoic acid **10a**. In the first experiment (Fig. 2) a THF solution of phenylpentadiynoic acid (**10a**) was treated with a slight excess of MsCl and pyridine (because one molecule of the dehydrating agent MsCl converts two molecules of acid to anhydride, 0.6 molar equivalents is actually a 1.2 stoichiometrically equivalent ratio and, hence, a "slight excess.") Within minutes even at 0 °C a precipitate as well as a blue, fluorescent TLC spot appeared. The latter was shown to be the product **11** following its isolation, indicating that we were in fact producing an HDDA benzyne at sub-ambient conditions! There was no evidence for the presumed intermediate anhydride. Also, there was no noticeable change in the TLC when the reaction mixture was allowed to further incubate overnight. The 4-chlorobutoxy group in **11** can be accounted for by the ring-opening of the oxonium ion **13**.[15] This, in turn, can arise from initial trapping of the HDDA benzyne **12** by THF at the more electrophilic carbon (C_β) followed by protonation at the carbon atom of the initially formed zwitterionic oxonium-carbanion.

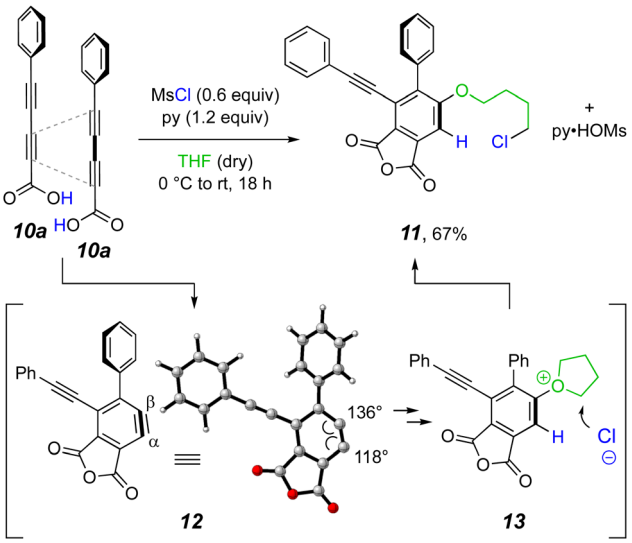

Fig. 2 Our first example of *in situ*, MsCl-promoted condensation of the diynoic acid **10a** (1.0 equiv.) to form an anhydride, which underwent rapid HDDA cycloisomerization. The intermediate electrophilic benzyne **12** was immediately trapped by a THF solvent molecule and the oxonium ion **13** was ring-opened by chloride ion.

By incubating **10a** with MsCl and pyridine in a non-interacting solvent (DCM instead of the THF used in Fig. 2), we were able to establish reaction conditions that allowed for generalized benzyne trapping. The first example employing these conditions used furan as an external trap (Fig. 3a). This led to formation of the oxanorbornadiene derivative **14a** in excellent yield. We observed that trifluoroacetic anhydride and methanesulfonic anhydride also were effective dehydrating agents, although we did not further explore this. As shown in Fig. 3b, this anhydride-HDDA process tolerates the presence of electron-rich and -poor aryl (**10b–d**), heteroaryl (**10e**), alkyl (**10f**), and silyl (**10g–h**) substituents on the terminus of the diyne carboxylic acid substrate.

We also used several other trapping agents (Fig. 3c): benzyl azide provided the triazole **15**; thioanisole gave the sulfides **17**; ethyl diazoacetate led to the pyrazole **19**; mesityl nitrile oxide gave the isoxazole **20**; a munchnone derivative gave rise to the isoindoles **21**; and the simple dienes *N*-Boc-pyrrole, cyclopentadiene, and anthracene afforded the [4 + 2] cycloadducts **22**, **23**, and **24** respectively. We note that the tetrayne-derived products that contain an arylethynyl substituent on the phthalic anhydride scaffold show blue fluorescence, which represents further opportunity for investigation.

Not surprisingly, the phthalic anhydride moiety in the products of these one-pot, *in situ*, anhydride assembly, cycloisomerization, and trapping cascades could be efficiently derivatized with primary amines to afford the phthalimide derivatives **25a–f** (Fig. 4).[16] Phthalic anhydrides are substrates for a considerable array of additional types of transformation.[16] A recent report of anti-bacterial activities of similar phthalimide derivatives against plant pathogens is an example of contemporary interest in this class of compound.[17]

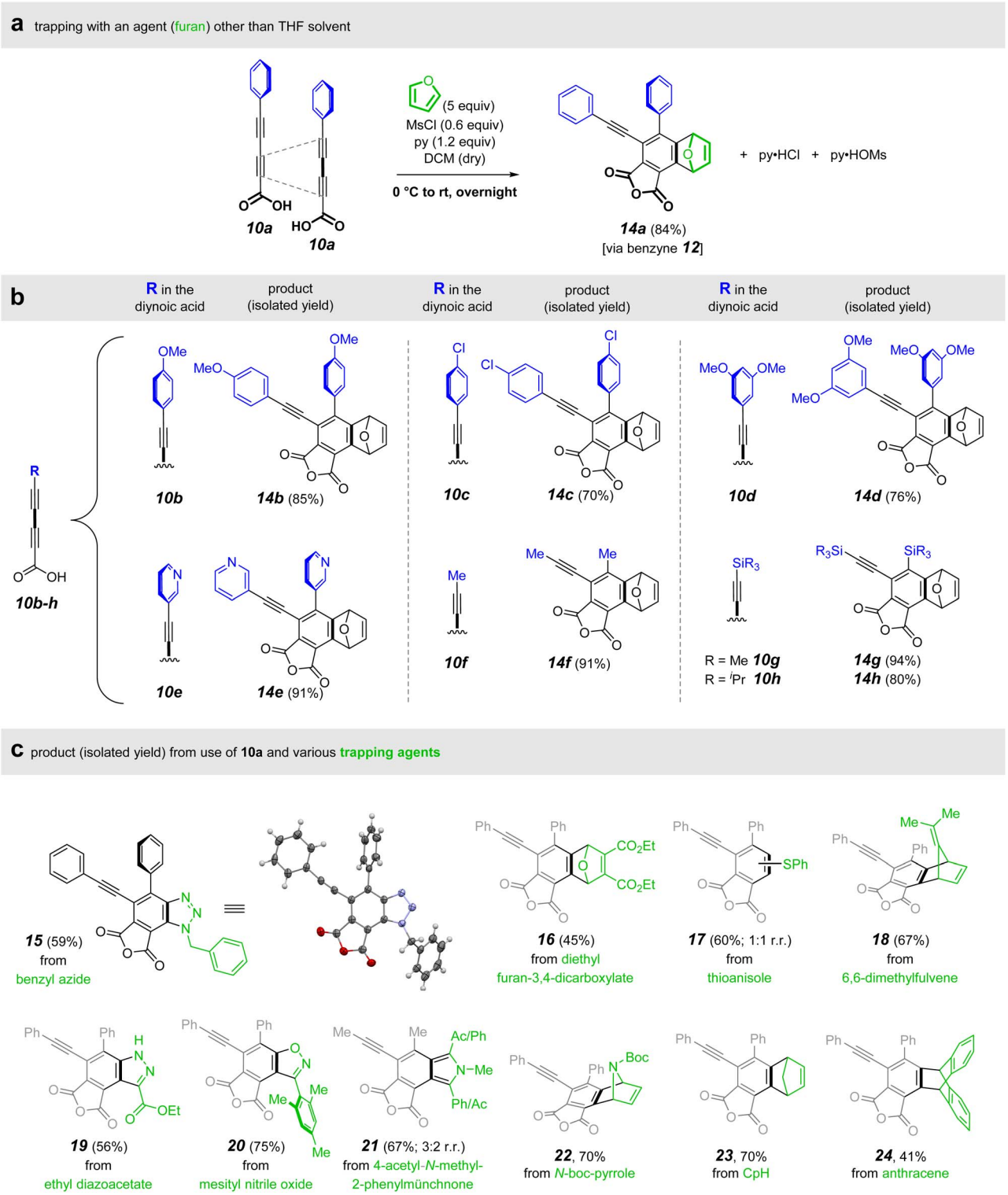

Fig. 3 (a) Furan trapping of the *in situ*-generated benzyne **12** derived from **10a**. A variety of (b) substituted diynoic acids **10b–h** (blue) and (c) benzyne trapping agents (green) are compatible with the *in situ* anhydride formation/HDDA cyclization conditions.

Recognizing that the applicability of this strategy would be enhanced if we could selectively make and cyclize mixed (*i.e.*, unsymmetric) anhydrides, we explored conditions that might allow this. Using the MsCl-mediated conditions for anhydride formation from a mixture of two different diynoic acids, one would expect, of course, a relatively non-selective formation of products from the three possible homo- and hetero-anhydrides. This was confirmed in a preliminary experiment (^{1}H NMR

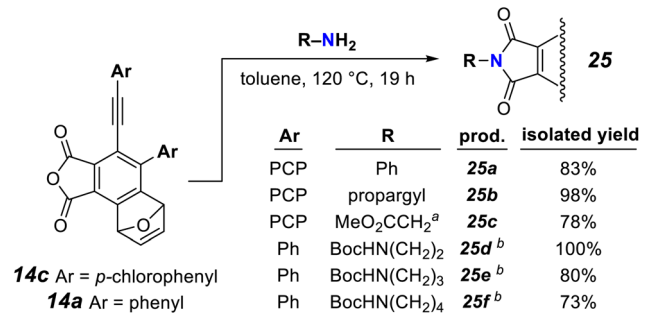

Ar	R	prod.	isolated yield
PCP	Ph	**25a**	83%
PCP	propargyl	**25b**	98%
PCP	MeO_2CCH_2 [a]	**25c**	78%
Ph	$BocHN(CH_2)_2$	**25d** [b]	100%
Ph	$BocHN(CH_2)_3$	**25e** [b]	80%
Ph	$BocHN(CH_2)_4$	**25f** [b]	73%

Fig. 4 Facile condensations of the phthalic anhydride moiety in **14a/c** with aniline, propargylamine, glycine methyl ester, and mono-boc diamines give imides **25a–f**. [a]Glycine methyl ester hydrochloride was used. [b]Yield is of the deprotected primary amine following subsequent Boc removal (TFA, rt, 30 min).

analysis of the crude product mixture[18]). Thus, we needed to find more-controlled, milder conditions for selectively forming a mixed anhydride that would persist sufficiently long for its HDDA cycloisomerization to take place. That is, conditions were needed that would not induce anhydride exchange of the unsymmetric anhydride, resulting in formation of unwanted symmetric anhydrides. We explored the use of an acid chloride/acid pair of substrates to generate the mixed anhydride. First, a dichloromethane solution of the preformed acid chloride **26** (structure in Fig. 5a) and the diyne acid **10f** was treated with a slight excess of pyridine. Again[18] we observed a more or less statistical mixture of the crossed and symmetrical products **27f**, **28f**, **14b**, and **14f**. This implied that pyridine and/or pyridinium chloride was catalyzing an unwanted anhydride metathesis event. We also examined the use of a silver(I) carboxylate salt to couple with the acid chloride **26**.[19] However, anhydride formation was thwarted by decarboxylation to give a terminal alkyne. We deemed other nucleophilic amine bases (*e.g.*, DBU, DMAP, or Et_3N) to be poor choices because of the susceptibility of ynoyl chlorides or anhydrides to undergo either 1,2- or 1,4-addition to the ynoyl moiety by species containing a basic nitrogen atom.

Finally, we chose to explore the use of Proton-sponge® [1,8-bis(dimethylamino)naphthalene], a less nucleophilic, yet more basic amine than pyridine.[20] This choice proved very rewarding (Fig. 5). Now the products derived from the unsymmetrical mixed anhydrides, arising from reaction of the acid chloride **26** with the acid **10f** or **10h**, were produced in good yield (Fig. 5b). Likewise, the triynes from **26** + **10i–k** were efficiently formed as shown by product formation. These results indicate that scrambling of the initial mixed anhydride was slower than its HDDA cyclization using Proton-sponge®. In the case of the mixed tetraynes, two different benzynes were formed, accounting for the formation of product pairs **27f**/**28f** and **27h**/**28h**.

The triynes derived from the propiolic acid derivatives **10i–k** also cyclized, now each to the furan adduct **27i–k** from trapping of the only possible benzyne intermediate. Notice that formation of the mesityl-containing product **27i** arises from an HDDA process even though a TDDA adduct could have been formed from the diradical intermediate common to both pathways. The

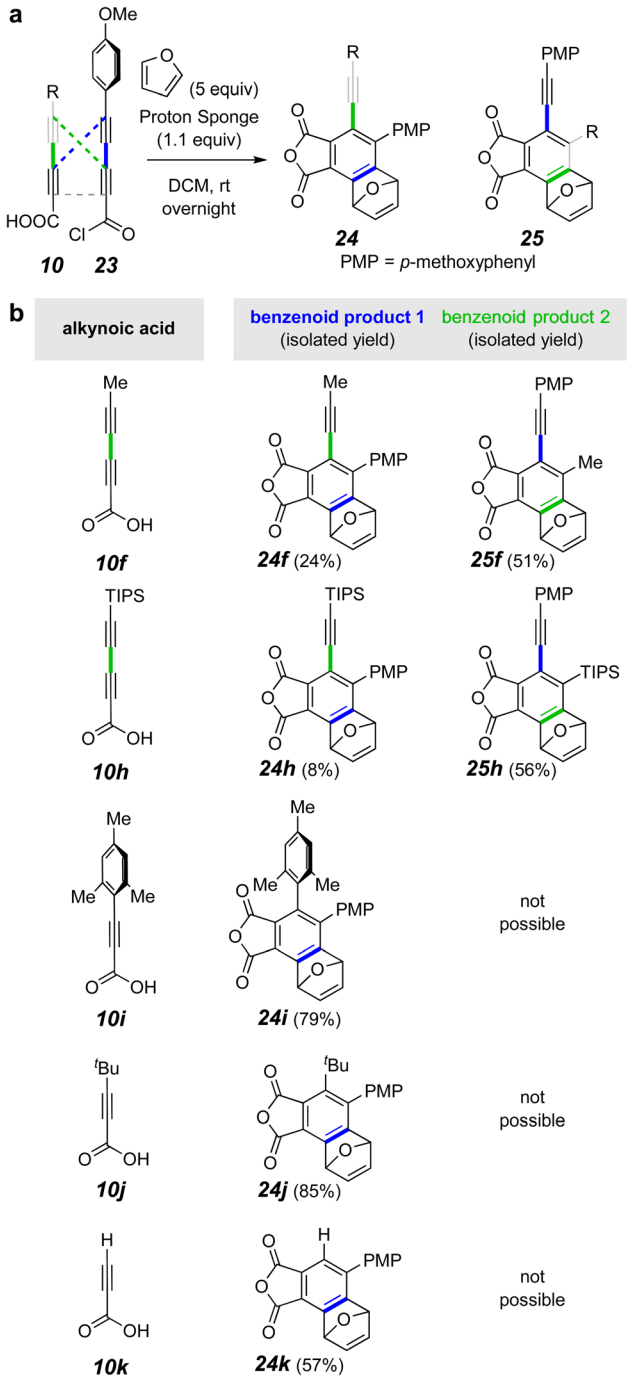

Fig. 5 (a) Generic representation of the preparation of mixed anhydrides using the acid chloride **26** to produce more varied product structure motifs. (b) Examples include unsymmetrical anhydride HDDA substrates of both tetrayne (**f**, **h**) and triyne (**i–k**) classes. [a]2.5 equiv. of **10k** used to minimize the amount of **14b** that was competitively formed.

presence of non-hydrogen substituents on C2 and C6 of the mesityl group significantly slows the TDDA mode of cyclization.[21]

A particularly striking result from the series of reactions involving of triyne anhydrides was the formation of **27k** from propiolic acid. To the best of our knowledge, this is the first

example of a triyne containing a terminal alkyne to undergo an HDDA cyclization at room temperature. The additional remote alkyne in a tetrayne enhances the rate of a HDDA cycloisomerization compared with an analogous triyne substrate.[22–24] This is because the additional radical stabilizing energy (RSE) of the alkyne lowers the barrier in the rate-limiting, benzyne-forming event.[25] Therefore, we wondered if the ability to make mixed anhydrides would provide an opportunity to now observe the formation of the triyne anhydride by *in situ* ^{1}H NMR analysis. Indeed, reaction of **10k** and **26** in $CDCl_3$ containing furan and Proton-sponge® allowed us to observe an acyclic anhydride (see **29a**, Fig. 6a) for the first time. This species appeared and competitively disappeared as a transient intermediate enroute to the furan-trapped product **27k**.

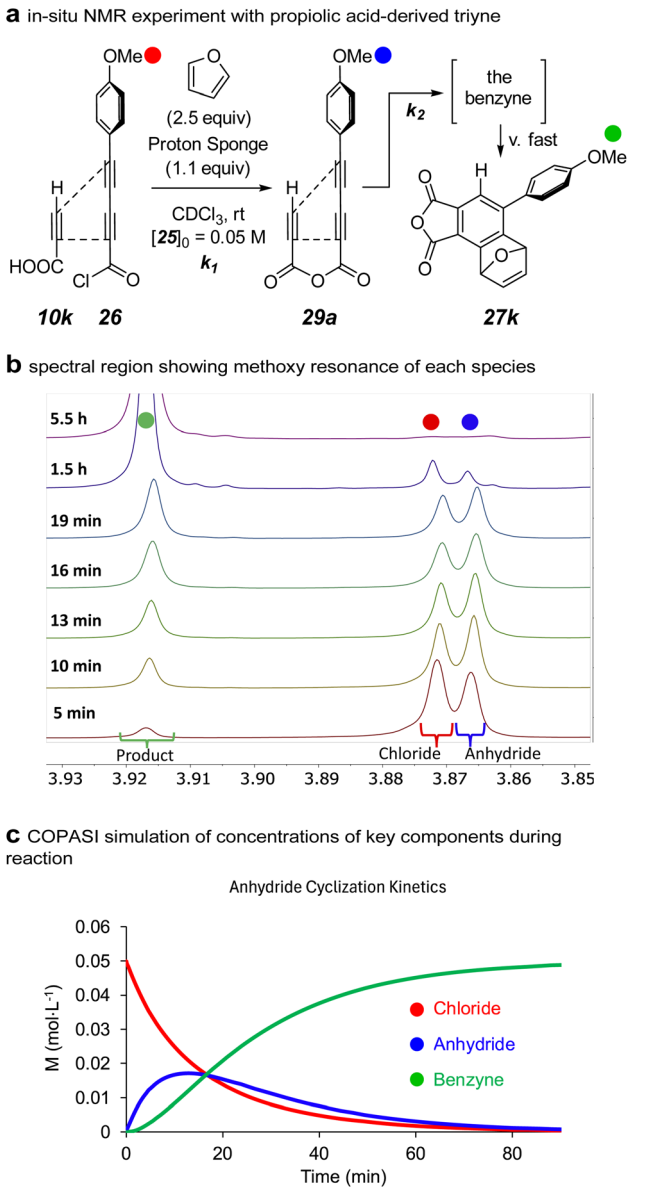

Fig. 6 (a) The reaction used to measure the half-life of HDDA cyclization of the anhydride intermediate **29a**. (b) *In situ* NMR data showing competitive formation and cyclization of the anhydride **29a**. (c) COPASI simulation of the first 90 min of data shown in panel b.

The ability to observe the mixed anhydride in the relatively less reactive triyne anhydride **29a** (from **10k** and **26**, Fig. 6a) meant that it should be possible to assess the magnitude of the rate enhancement afforded by the anhydride linkage. A stack plot of spectra over time shows changes in the methoxy resonances of the PMP groups in the acid chloride, mixed anhydride, and final product **26**, **29a**, and **27k**, respectively (Fig. 6b). Under the indicated conditions, the rate of formation of the anhydride, a bimolecular process, was observed to compete with that of its cyclization to the benzyne, which is not observed, of course, because of its extremely fast reaction with furan. The changes in the relative amounts of the three PMP-containing species over time were simulated with COPASI,[26] which provided the data represented in Fig. 6c. From this the extracted half-life for the HDDA cyclization of **29a** to the benzyne was 9 minutes.

We next asked how the rate of the anhydride linked substrate **29a** compared with that of the analogous ester- and ether-containing substrates **29b**/**c** and **29d** (Fig. 7). Because these latter three all cycloisomerize much more slowly than the anhydride analog, each was easily synthesized and purified. Each was then first converted preparatively into the HDDA benzyne-trapped products **30b**/**c** (from reaction with furan) and **30d** (from reaction with cyclooctane[27]).

With NMR data for authentic samples of products **30b–d** in hand, we proceeded to measure the half-life for the rate-limiting cycloisomerization of each of the triynes **29b–d** in $CDCl_3$ (see ESI† for the detailed protocol). Using a convenient temperature

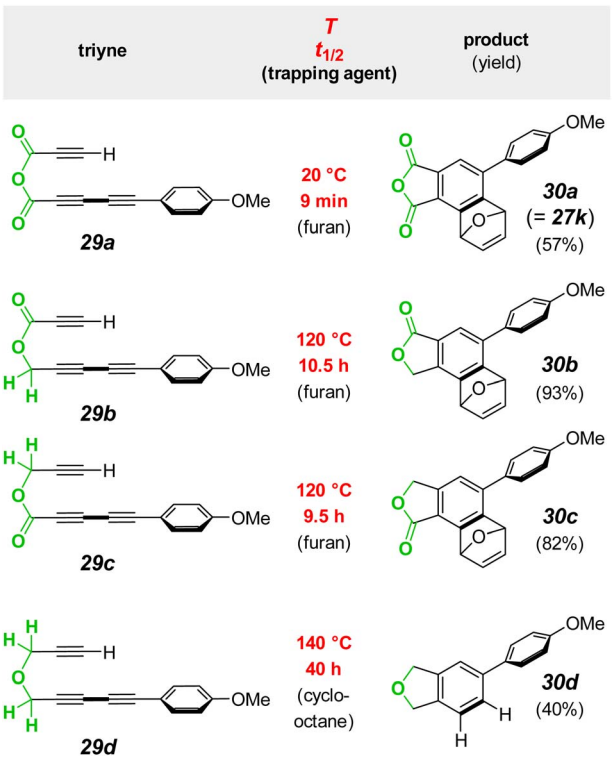

Fig. 7 Large rate enhancement (red) for the HDDA cyclization of the triyne **29a** having an anhydride tether compared to the rates of substates **29b–d** having ester or ether tethers.

for the reaction rate of these much less reactive substrates (relative to the anhydride **29a**), we used NMR spectroscopy to monitor the disappearance of each. The half -lives at 120 °C for **29b** and **29c** were very similar to one another (10.5 and 9.5 h, respectively) as well as to that seen for an analog of **29b** in an earlier study.[13,23] Substrate **29d** having the ether linkage proved to be even less reactive. (All of the measured half-lives for **29a–d** are also listed in column two of the tabulated data in Fig. 8b).

Clearly, the anhydride linker present in substrate **29a** and, by extension, all of the other anhydrides involved in the reactions in Fig. 2, 3, and 5 are imparting a dramatic rate-acceleration on the HDDA cycloisomerization. Why? To address this question, we carried out a revealing distortion/interaction (aka, activation strain) analysis (Fig. 8a).[28] Generally speaking and in the well-stated words of Bickelhaupt and Houk, "the activation strain or distortion/interaction model is a tool to analyze activation barriers that determine reaction rates. For bimolecular reactions, the activation energies are the sum of the energies to distort the reactants into geometries they have in transition states plus the interaction energies between the two distorted molecules. The energy required to distort the molecules is called the activation strain or distortion energy. This energy is the principal contributor to the activation barrier. The transition state occurs when this activation strain is overcome by the stabilizing interaction energy."[28]

The specific approach used here involved first computing the energetic barrier for the initial C–C bond formation in each of **29a–d** leading to the corresponding diradical (see ESI†) enroute to each benzyne. These computed activation energies ($\Delta E^{\ddagger}$) are given in column 3 of Fig. 8b. They correlate well with the approximate relative rates of reaction of each of these four substrates (extrapolated from their reactions at different temperatures[29]). The tethering atoms in each computed structure of **31a–d**‡ were then excised and replaced by a hydrogen atom to give rise to the four different structures of **34**‡.[30] In each of these, the internuclear distance l in **31**‡ is maintained. The two "halves" of **31**‡ were then separated to infinite distance, giving $\mathbf{32_{dist}}$ and $\mathbf{33_{dist}}$, the distorted but non-interacting, free alkyne components. To identify the distortion energy developed in the transition structures (TSs) **31**‡, the tether was also excised from **32** to produce, following optimization, the undistorted alkyne components **32** and **33**. The difference in (the single point) energies between $\mathbf{32_{dist}}$ *vs.* **32** and $\mathbf{33_{dist}}$ *vs.* **33** comprise the total distortion energy ($\Delta E^{\ddagger}_{\mathrm{dist}}$) Likewise, the difference in energy between **34**‡ and $\mathbf{32_{dist}}$ + $\mathbf{33_{dist}}$ gives the interaction energy for each of the four analogs.

Notably, the values of both the $\Delta E^{\ddagger}_{\mathrm{dist}}$ and the $\Delta E^{\ddagger}_{\mathrm{int}}$ [as well as, therefore, their sum $\Delta E^{\ddagger}_{\mathrm{total}}$] were nearly identical for all four sets of structures (columns 4–6, Fig. 8b). Moreover, the interaction energy in **34**‡ for each of the four reactions was destabilizing. This is an uncommon, but not unprecedented,[31] phenomenon, including an example seen for a computed, stepwise HDDA reaction.[32] The implication is that at the distances and geometries between the alkyne moieties in **34**‡ (and **31**‡), the alkynes have more destabilizing, repulsive interaction than stabilizing, bonding interaction. The energetic contribution imposed/provided by the tether $\Delta E^{\ddagger}_{\mathrm{teth}}$ is, therefore, the difference in activation energies between the intact tethered substrates **29a–d** proceeding to **31a–d**‡ ($\Delta E^{\ddagger}$) *vs.* the untethered analogs **32** and **33** proceeding to **34a–d**‡ $\Delta E^{\ddagger}_{\mathrm{total}}$.

These are significantly different across the series of tethers (column 7, Fig. 8b). Relative to the ether in **29d**, the anhydride in **29a** provides *ca.* 10 kcal mol^{-1} greater stabilization to its transition structure.

At a more fundamental level, the question remains: why is the anhydride so different? Two factors may be contributing. First, nearly all acyclic anhydrides, including the HDDA substrates here, are composed (as judged by computation as well as microwave and rotational–vibrational spectroscopies) of a family of non-coplanar conformations[33] (the exception being formic anhydride[34]). In the phthalic anhydride products produced here, the enforced planarity of the anhydride could lead to a greater degree of stabilization (resonance and/or

a initial bond formation in tethered triynes **29** and *distortion/interaction* analysis

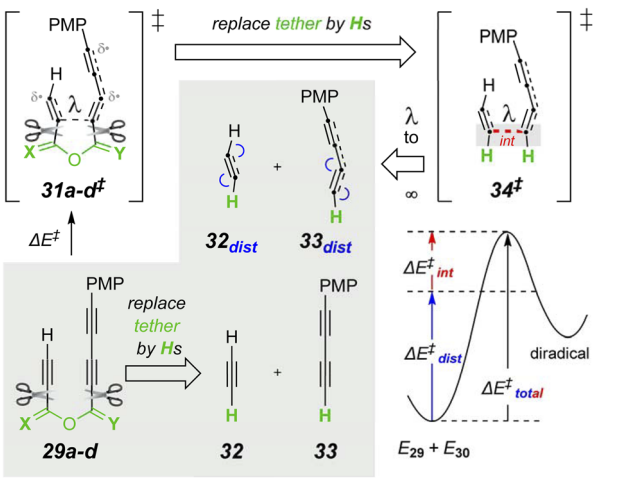

b $t_{1/2}$s and parameters from *distortion/interaction* analysis (*E*s in kcal mol^{-1})

X and Y	$t_{1/2}$ experimental	intact tethered triyne $\Delta E^{\ddagger}$ =	contribution from: triyne alone $\Delta E^{\ddagger}_{total}$	$\Delta E^{\ddagger}_{dist}$	$\Delta E^{\ddagger}_{int}$	tether alone $\Delta E^{\ddagger}_{teth}$	λ (Å) in 31‡
X = Y = O **29a**	9 min (20 °C)	19.3	29.1	23.7	5.4	-9.7	1.88
X = O; Y = H_2 **29b**	10.5 h (120 °C)	24.8	28.8	24.5	4.3	-4.0	1.83
X = H_2; Y = O **29c**	9.5 h (120 °C)	26.0	28.9	23.2	5.7	-2.9	1.83
X = Y = H_2 **29d**	40 h (140 °C)	29.2	28.9	24.6	4.3	0.4	1.82

Fig. 8 (a) Distortion/interaction analysis performed on the series of tethered triynes **29a–d**. (b) Experimental half-lives and DFT[a]-computed parameters[b] separating the energetic contributions from the triyne *vs.* those from the tether components to the overall barrier height for the initial, rate-limiting C–C bond formation in each of the triynes **29a–d**. [a][(U)B3LYP-GD3BJ/6-311+G(d,p), SMD: chloroform]. [b]$\Delta E^{\ddagger} = E_{31\ddagger} - E_{32} \| \Delta E^{\ddagger}_{\mathrm{total}} = E_{34\ddagger} - (E_{32} + E_{33}) \| \Delta E^{\ddagger}_{\mathrm{dist}} = (E_{32\mathrm{dist}} + E_{33\mathrm{dist}}) - (E_{32} + E_{33}) \| \Delta E^{\ddagger}_{\mathrm{int}} = \Delta E^{\ddagger}_{\mathrm{total}} - \Delta E^{\ddagger}_{\mathrm{dist}} \| \Delta E^{\ddagger}_{\mathrm{teth}} = \Delta E^{\ddagger} - \Delta E^{\ddagger}_{\mathrm{total}}$.

strain?)[35] relative to the ester-to-lactone and ether-to-ether cyclizations. To probe that possibility, we examined the simple set of homodesmotic reactions (note the same number and type of functional groups on each side of the reaction equation) shown in Fig. 9. The enthalpy change between the (all-anti conformer of the) ring-opened *vs.* the ring-closed forms for each of the three functional groups (*i.e.*, ether, *vs.* ester, *vs.* anhydride) was computed with DFT. The magnitudes of the differences in the ΔH's across this series of cyclizations correlate well with the differences in the rates of the HDDA cyclizations. This reinforces the conclusions from the distortion/interaction analysis. That is, that the primary differentiating factor in the large differences in reactivity for the series **29a–d** is the enthalpy change associated with each tether as it undergoes the cyclization, the anhydride being uniquely favorable.

Finally, a 2023 report from the Chen and Li groups at Guizhou University describes a robust method for preparing symmetrical *N*,*N*-bis-(3-aryl)propiolylimides that cyclize at ambient temperature to give naphthalimide derivatives **38** (Fig. 10a).[17] Precursor amines **35** were acylated with two equivalents each of an arylpropiolic acid **36** and *N*,*N*′-diisopropylcarbodiimide (DIC). The intermediate imides **37** spontaneously underwent a TDDA reaction (*cf.* Fig. 1a) to produce products **38** in very good to excellent yields. Over four dozen examples were reported. All reactions were performed at ambient temperature for 24 h.

A reviewer of our manuscript asked whether there was any other type of linker that would accelerate a cyclization by virtue of the planarization phenomenon seen with the anhydride. Because the imide-templated reaction from Chen and Li represents such a linker and especially because it bears

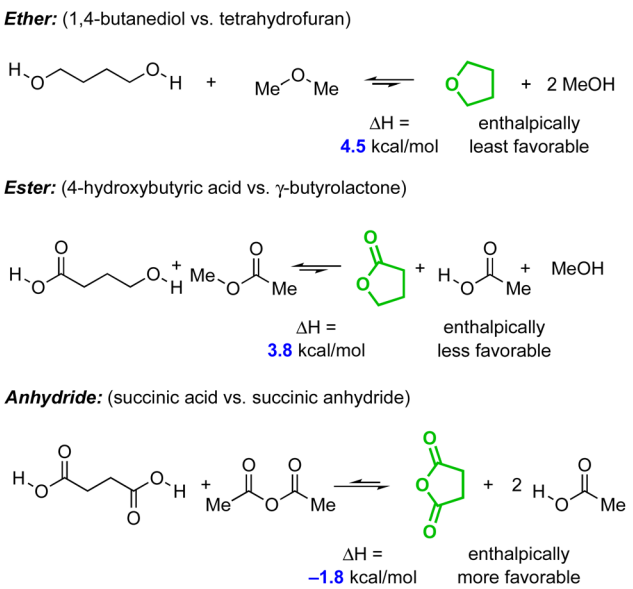

Fig. 9 Computed[a] enthalpic change for a series of homodesmotic reactions showing the unique favorability (−1.8 kcal mol^{-1}) afforded by conversion of the acyclic to cyclic anhydride compared to the unfavorable enthalpies of cyclization for the ether and ester analogs (+4.5 and +3.8 kcal mol^{-1}, respectively). [a][(MN15/6-311++G(d,p), SMD : water].

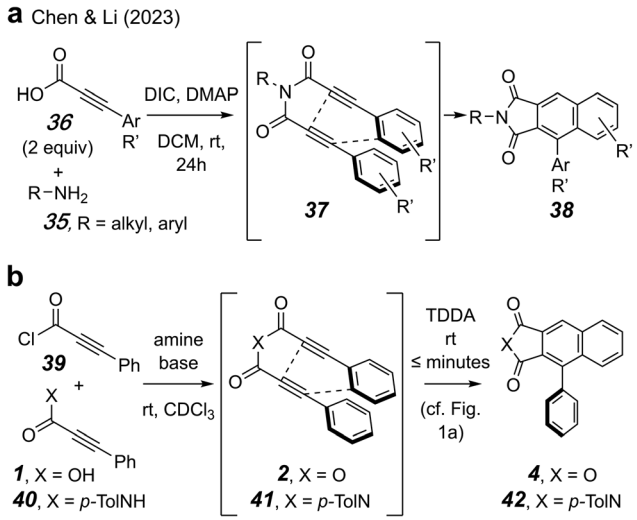

Fig. 10 Tetradehydro-Diels–Alder (TDDA) reactions of propiolic acid chloride-derived anhydride- and imide-linked TDDA substrates **2** and **37**. The imide cyclizes faster than the anhydride.

considerable similarity to the anhydride work disclosed here, we were curious about the actual extent to which an imide would accelerate this type of cycloisomerization. Toward that end, we prepared, *in situ*, the symmetrical TDDA substrates, phenylpropiolic anhydride (**2**) and *N*-(*p*-tolyl)-*N*,*N*-bis-(3-phenylpropiolyl)imide (**41**) (Fig. 10b). We used ^{1}H NMR spectroscopy to monitor reactions in $CDCl_3$ between phenylpropiolic acid chloride (**39**) with either 3-phenylpropiolic acid (**1**) in the presence of Proton-sponge® or 3-phenyl-*N*-(*p*-tolyl)propiolamide (**40**) in the presence DMAP/Et_3N.[36] The rate of the TDDA cycloisomerization of the imide **41** to produce the naphthalimide derivative **42** was significantly faster than that of the anhydride **2** to give **4** (see ESI†). Further studies to more fully evaluate and quantify the extent of this even greater rate acceleration by an imide are planned. We note in closing that this strategy for imide formation is readily amenable to the preparation of unsymmetrical *N*,*N*-bis-(propiolyl)imides.

Conclusion

We have demonstrated here the first example of HDDA cycloisomerization of a poly-yne precursor possessing an anhydride linker *via* dehydration of shelf-stable carboxylic acid diynes. Substrates containing the anhydride have proven to show much higher than expected cyclization rates. In accordance with, a perhaps underappreciated, 50[10]–125[2] year-old precedent of the facile TDDA reaction of phenylpropiolic acid anhydride (Fig. 1a), the HDDA variant produces benzyne at or below room temperature (including, for the first time, a substrate having a terminal propargylic alkyne serving as the diynophile). This expands the scope of conditions under which HDDA-benzyne formation and trapping can be performed. Use of MsCl as a dehydrating agent at room temperature leads to formation of symmetric anhydrides derived from dimerization of a variety of diynoic acids. These quickly proceed to benzyne formation and

in situ trapping to form various phthalic anhydride derivatives, including a number with fused heterocyclic moieties. Post-HDDA modifications of several of the phthalic anhydride products to their phthalimide derivatives demonstrate the ease with which potential other polar moieties can be introduced. By employing a diynoic acid chloride, we further identified conditions that allowed for selective formation of the benzyne derived from mixed anhydrides, further expanding the modularity of the approach.

We also deduced the reason for the rate enhancement afforded by the anhydride linker. By synthesizing a series of triyne substrates that varied only in their linker structure (ether, ester, and anhydride), we found that the rate of HDDA cycloisomerization increased, dramatically, in the stated order (estimated to be $>10^7$ compared to the analogous ether-linked substrate[29]). To rationalize this trend, we performed a distortion/interaction analysis that revealed that: (i) the distortion/interaction within the diyne–diynophile reacting atoms was nearly identical for all three classes of substrate, and (ii) all four substrates have a destabilizing (*i.e.*, positive) interaction energy at the internuclear distance present in the computed transition structure of each.

A series of simple homodesmotic calculations were performed to assess the enthalpy difference between ring-opened *vs.* -closed forms for THF, γ-butyrolactone, and succinic anhydride. This showed that it is the energetic contribution associated with the formation of the fused, cyclic five-membered anhydride in the benzyne intermediate that is the principal contributor to the substantially higher rate of the HDDA cycloisomerization. Thus, the differences in stabilization of the transition structures across the series of four substrate classes arise nearly entirely from changes within the reorganization of the tethering atoms. This understanding explains why that, in this setting, the anhydride tether is a kinetically privileged linker. Finally, we have observed that an *N*-aryl imide analog of the anhydride linker induces an even greater rate acceleration.

Data availability

The data upon which the conclusions in this manuscript are based are provided in the ESI† document and in a .zip file of a master Mnova file of all NMR spectra.

Author contributions

D. S. S. conceived the project, effected the initial examples, and carried out the computational studies, D. S. S. and P. V. K. carried out similar amounts of the experimentation, and all three authors analyzed the data and co-wrote the manuscript.

Conflicts of interest

There are no conflicts to declare.

Acknowledgements

This study was made possible by a research grant from the National Institutes of General Medical Sciences (R35 GM127097), part of the U.S. Department of Health and Human Services. D. S. S. was supported by a Wayland E. Noland Excellence Fellowship. A portion of the NMR spectral data were collected using an instrument partially funded by the Shared Instrumentation Grant program (S10 OD011952) of the National Institutes of Health. ESI HRMS data were obtained at the Masonic Cancer Center (Analytical Biochemistry Shared Resource laboratory) at the University of Minnesota; the instrumentation there was partially funded by the NIH Cancer Center Support Grant (P30 CA77598). The X-ray diffraction data were collected using an instrument purchased with the support of the National Science Foundation (NSF/MRI 1229400). The DFT computational studies were performed using the facilities of the University of Minnesota Supercomputing Institute (MSI). Alex Lovstedt (Department of Chemistry, University of Minnesota) is thanked for performing the X-ray diffraction analysis.

Notes and references

1 P. Wessig and G. Müller, *Chem. Rev.*, 2008, **108**, 2051–2063.
2 A. Michael and J. E. Bucher, *Chem. Ber.*, 1895, (28), 2511–2512.
3 A. Michael and J. E. Bucher, *Am. Chem. J.*, 1898, **20**, 89–127.
4 T. Lanser, *Chem. Ber.*, 1899, (32), 2478–2481.
5 F. G. Baddar and L. S. El-Assal, *J. Chem. Soc.*, 1948, 1267–1270.
6 This type of process was demonstrated to proceed *via* a cyclic allene: R. L. Danheiser, A. E. Gould, R. F. de la Pradilla and A. L. Helgason, *J. Org. Chem.*, 1994, **59**, 5514–5515.
7 O. Diels and K. Alder, *Justus Liebigs Ann. Chem.*, 1928, **460**, 98–122.
8 (*a*) K. Miyawaki, R. Suzuki, T. Kawano and I. Ueda, *Tetrahedron Lett.*, 1997, **38**, 3943–3946; (*b*) A. Z. Bradley and R. , P. Johnson, *J. Am. Chem. Soc.*, 1997, **119**, 9917–9918; (*c*) T. R. Hoye, B. Baire, D. Niu, P. H. Willoughby and B. P. Woods, *Nature*, 2012, **490**, 208–211.
9 W. Xu, X. Li, L. Zou, X. Li, Z. Zhang, A. Ali, Z. Wang, P. Li and H. Zheng, *J. Org. Chem.*, 2023, **88**, 208–212.
10 P. A. Cadby, M. T. Hearn and A. D. Ward, *Aust. J. Chem.*, 1973, **26**, 557–570.
11 This evolution of reports of the temperatures used to effect the transformation of **2** to **4** serves as a reminder to an occasionally overlooked reality that a published experimental procedure reports what the researcher did, but not necessarily whether they needed to do so (time, temperature, reactant stoichiometry, concentration, catalyst load, *etc.*).
12 A. Ajaz, A. Z. Bradley, R. C. Burrell, W. Hoi Hong Li, K. J. Daoust, L. B. Bovee, K. J. DiRico and R. P. Johnson, *J. Org. Chem.*, 2011, **76**, 9320–9328.
13 (*a*) B. P. Woods, B. Baire and T. R. Hoye, *Org. Lett.*, 2014, **16**, 4578–4581; (*b*) R. Karmakar and D. Lee, *Org. Lett.*, 2016, **18**, 6105–6107; (*c*) S. Yoshida, K. Shimizu, K. Uchida, Y. Hazama,

K. Igawa, K. Tomooka and T. Hosoya, *Chem.–Eur. J.*, 2017, **23**, 15332–15335; (*d*) C. Zhu and T. R. Hoye, *J. Am. Chem. Soc.*, 2022, **144**, 7750–7757.

14 K. C. Nicolaou, P. S. Baran, Y. Zhong, H. Choi, K. C. Fong, Y. He and W. H. Yoon, *Org. Lett.*, 1999, **1**, 883–886.

15 M. A. Birkett, D. W. Knight, P. B. Little and M. B. Mitchell, *Tetrahedron*, 2000, **56**, 1013–1023.

16 For recent overviews that describe phthalimide chemistries, see: (*a*) R. A. Aitken, Synthesis of cyclic imides, in *Imides: Medicinal, Agricultural, Synthetic Applications, and Natural Products Chemistry*, ed. F. A. Luzzio, Elsevier, 2019, ch. 1, pp. 1–28; (*b*) K. Nikoofar and M. Sadathosainy, *RSC Adv.*, 2023, **13**, 23870–23946.

17 C. Song, T. Shen, L. Chen and T. Li, *Org. Chem. Front.*, 2023, **10**, 3792–3798.

18 An equimolar mixture of the diyne acids **10b** and **10f** was treated under the conditions used in Fig. 3 [with MsCl (0.6 equiv.) and pyridine (1.2 equiv.) in DCM] to produce **14b**, **14f**, **27f**, and **28f** in a ratio of 2.3 : 2.0 : 1.2 : 3.0 (see Fig. 5 for the structures of **27f** and **28f** from the intermediate unsymmetric anhydride).

19 There are multiple reports of this reaction being used to prepare anhydrides with non-alkynoic acid substrates since its original disclosure: A. R. Ferris and W. D. Emmons, *J. Am. Chem. Soc.*, 1953, **75**, 232–233.

20 pK_a of Proton-sponge® = 12.3: R. W. Alder, P. S. Bowman, W. R. S. Steele and D. R. Winterman, *J. Chem. Soc., Chem. Commun.*, 1968, 723–724.

21 For an example of cycloisomerization of a triyne substrate having an unsubstituted phenyl substituent on the diynophile that preferentially follows the TDDA pathway see: D. Rodríguez, L. Castedo, D. Domínguez and C. Saá, *Tetrahedron Lett.*, 1999, **40**, 7701–7704.

22 L. L. Fluegel and T. R. Hoye, *Chem. Rev.*, 2021, **121**, 2413–2444.

23 Y. Liang, X. Hong, P. Yu and K. N. Houk, *Org. Lett.*, 2014, **16**, 5702–5705.

24 D. J. Marell, L. R. Furan, B. P. Woods, X. Lei, A. J. Bendelsmith, C. J. Cramer, T. R. Hoye and K. T. Kuwata, *J. Org. Chem.*, 2015, **80**, 11744–11754.

25 T. Wang, D. Niu and T. R. Hoye, *J. Am. Chem. Soc.*, 2016, **138**, 7832–7835.

26 S. Hoops, S. Sahle, R. Gauge, C. Lee, J. Pahle, N. Simus, M. Singhal, L. Xu, P. Mendes and U. Kummer, *Bioinformatics*, 2006, **22**, 3067–3074.

27 D. Niu, P. H. Willoughby, B. Baire, B. P. Woods and T. R. Hoye, *Nature*, 2013, **501**, 531–534.

28 F. M. Bickelhaupt and K. N. Houk, *Angew. Chem., Int. Ed.*, 2017, **56**, 10070–10086.

29 Under the assumption that the reaction rate for the rate-determining step in these HDDA reactions is enhanced by 2.5x for each increase of 10 °C in the reaction temperature, the reaction rates range for the slowest (ether) to fastest (anhydride) substrates by a krel of 1.5×10^7.

30 For an example of a distortion/interaction treatment of an intramolecular cycloaddition, see E. H. Krenske, K. N. Houk, A. B. Holmes and J. Thompson, *Tetrahedron Lett.*, 2011, **52**, 2181–2184.

31 A positive interaction energy at or leading to a transition structure has been demonstrated in reactions such as: (*a*) Carbene addition to alkynes. C. A. Sader and K. N. Houk, *Arkivoc*, 2014, **2014**, 170–183; (*b*) Double group transfer reactions. I. Fernández, F. M. Bickelhaupt and F. P. Cossío, *Chem.–Eur. J.*, 2009, **15**, 13022–13032; (*c*) Alder-ene reactions. I. Fernández and F. M. Bickelhaupt, *J. Comput. Chem.*, 2012, **33**, 509–516; (*d*) (3+2) Cycloadditions. I. Fernández, F. P. Cossío and F. M. Bickelhaupt, *J. Org. Chem.*, 2011, **76**, 2310–2314.

32 Y. Liang, X. Hong, P. Yu and K. N. Houk, *Org. Lett.*, 2014, **16**, 5702–5705.

33 (*a*) G. Wu, C. Van Alsenoy, H. J. Geise, E. Sluyts, B. J. Van der Veken, I. F. Shishkov and L. V. Khristenko, *J. Phys. Chem. A*, 2000, **104**, 1576–1587; (*b*) N. Love, A. J. Reynolds, M. A. Dvorak and K. R. Leopold, *J. Mol. Spectrosc.*, 2023, **397**, 111844; (*c*) N. Love, K. J. Koziol, K. Belmont and K. R. Leopold, *J. Mol. Spectrosc.*, 2024, **403**, 111926.

34 Formic anhydride is computed to have two co-planar conformers (W-, and S-shaped) and third nearly coplanar (U-shaped)(*a*) N. Myllys, I. Osadchuk and J. Lundell, *J. Mol. Struct.*, 2024, **1304**, 137643; (*b*) G. Wu, S. Shlykov, F. S. Van Alseny, H. J. Geise, E. Sluyts and B. J. Van der Veken, *J. Phys. Chem.*, 1995, **99**, 8589–8598.

35 J. B. Conn, G. B. Kistiakowsky, R. M. Roberts and E. A. Smith, *J. Am. Chem. Soc.*, 1942, **64**, 1747–1752.

36 Y. Zhang, H. Ma, Y. Wu, Z. Wu, Z. Yao, W. Zhang, C. Zhuang and Z. Miao, *Bioorg. Med. Chem. Lett.*, 2017, **27**, 2308–2312.